VOL. 10, NO. 14, AUGUST 2015 ISSN 1819-6608
ARPN Journal of Engineering and Applied Sciences

www.arpnjournals.com

MAGNETO-HYDRODYNAMICS NON-NEWTONIAN SQUEEZE FILM CHARACTERISTICS OF POROUS CURVED CIRCULAR PLATES

Santhana Krishnan Narayanan and Sundarammal Kesavan
Department of Mathematics, SRM University, Kattankulathur, Tamilnadu, India
E-Mail: sundarammal@gmail.com

ABSTRACT

The squeeze film characteristics between porous curved circular plates lubricated with an electrically conducting non-Newtonian fluid in the presence of an external magnetic field are investigated in this paper. Based upon the Magneto-hydrodynamic flow theory together with the Stokes micro-continuum theory, the magneto-hydrodynamic non-Newtonian (MHNN) Reynolds equation is derived and applied to predict the porous curved circular squeeze film behaviours. The expressions for MHNN porous squeeze film pressure, load-carrying capacity and squeeze film time are obtained. Comparing with the hydrodynamic Newtonian case, the squeeze film characteristics for porous curved circular plates are improved by the use of an electrically conducting non-Newtonian fluid in the presence of external magnetic fields.

Keywords: MHNN characteristics, porous squeeze film, curved circular plates, electrically conducting fluid.

1. INTRODUCTION

With the rapid development of modern equipment machines, the increasing use of fluids containing microstructures such as additives, suspensions and long-chained polymers has received great attention. The porous squeeze film technology plays an important role in many areas of engineering practice and applied science. Due to the change of temperature, an unexpected variation of lubricant viscosity occurs. To prevent this, an increasing use of an electrically conducting fluid as the lubricant with an external magnetic field has become of common interest. In the presence of an external magnetic fluid, the load-carrying capacity of Magneto-hydrodynamics (MHD) porous squeeze films is increased.

Several studies have investigated the MHD effects on the lubrication performances of the journal bearings by Malik and Singh [1], the slider bearings by Lin [2] and squeeze film bearings by Lin et al [3]. The presence of additives is found to have beneficial effects on the load-carrying capacity and bearing characteristics by the experimental works by Oliver [4]. Several articles have applied this non-Newtonian (NN) model of couple stress fluids to investigate various squeeze film systems, such as the squeeze film mechanism with reference to human joints by Ahmad and Singh [5] and sphere-plate film by Elsharkarsy and AL-Fadhalah [6]. According to their results, the NN influences of couple stresses increase the load-carrying capacity and lengthen the response time for squeeze films. From the above studies, when an electrically conducting fluid is mixed with small amount of long-chained additives, the NN effects of couple stresses would apper in squeeze film. Traditionally, the analysis of porous squeeze film bearings was based on the Darcy's model, where the fluid flow in the porous matrix obeys Darcy's law and at the case of two approaching surfaces which attempt to displace a viscous fluid between them. If one (or) both of the approaching surfaces are porous, the lubricant not only get squeezed out from the sides but also bleeds into the pores of the porous matrix, thus reducing the time of approach of the surfaces considerably. Despite this advantage, porous bearing have proved to be useful because of their design simplicity and self-lubricating characteristics.

According to the recent study on the Magneto-hydrodynamic non-Newtonian (MHNN) curved circular squeeze film by Lin *et al* [7]; the curved mechanism is imported for engineering application. Therefore, a further investigation is motivated in the present study for porous squeeze film characteristics in MHNN curved circular plates. The porous squeeze film characteristics between curved circular plates lubricated with an electrically conducting non-Newtonian fluid in the presence of an external magnetic field are investigated in this paper. Based upon the Magneto-hydrodynamic flow theory together with the Stokes micro-continuum theory, the magneto-hydrodynamic non-Newtonian (MHNN) Reynolds equation is derived and applied to predict the porous curved circular squeeze film behaviours. The expressions for MHNN porous squeeze film pressure, load-carrying capacity and squeeze film time are obtained. Comparing with the hydrodynamic Newtonian case, the squeeze film characteristics for porous curved circular plates are improved by the use of an electrically conducting non-Newtonian fluid in the presence of external magnetic fields.

2. MATHEMATICAL FORMULATION OF THE PROBLEM

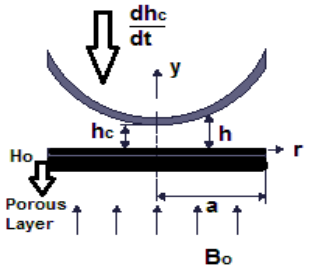

Figure-1. Geometry of MHNN porous squeeze film curved circular plates in the presence of a transverse uniform magnetic field.

Figure-1 describes the porous squeeze film geometry between upper curved circular plates of radius a is approaching the bottom fixed plate of porous bearing of wall thickness H_o with a velocity $\frac{\partial h_c}{\partial t}$ under a constant load. The porous region is lubricated with an electrically conducting non-Newtonian couple-stress fluid. An external magnetic field B_o is applied in y-direction. The film shape h is taken to be an exponential type as Murti [8].

$$h = h_c \exp\left(\frac{-kr^2}{a^2}\right) \tag{1}$$

where h_c is the central minimum film thickness and k is the curved shape parameter. Assume that the thin film lubrication theory as Hamrock [9] is applicable and the induced magnetic field is small when comparing with the magnetic field. Following the MHD flow equation of Lin [2] and the stokes microcontinuum theory [10], the Magneto-hydrodynamic Non-Newtonian (MHNN) couple stress momentum equations and the continuity equation can be expressed in axially cylindrical coordinates as follows.

$$\frac{\partial p}{\partial r} = \mu\frac{\partial^2 u}{\partial y^2} - \eta\frac{\partial^4 u}{\partial y^4} - \sigma B_o^2 u \tag{2}$$

$$\frac{\partial p}{\partial y} = 0 \tag{3}$$

$$\frac{1}{r}\frac{\partial (ru)}{\partial r} + \frac{\partial v}{\partial y} = 0 \tag{4}$$

where p is the hydrodynamic film pressure, u and v are the velocity components in the r- and y- directions respectively, μ is the lubricant viscosity, σ denotes the electrical conductivity of the lubricant and η represents a material constant responsible for the non-Newtonian couple stress fluid. The flow of conducting lubricant in the porous region is governed by the modified Darcy's law [11].

$$u^* = -\frac{k'}{\mu}\frac{\partial p^*}{\partial r}\frac{1}{c'^2} \tag{5}$$

$$v^* = -\frac{k'}{\mu(1-\beta)}\frac{\partial p^*}{\partial y}$$

$$\frac{1}{r}\frac{\partial}{\partial r}\left(ru^*\right) + \frac{\partial v^*}{\partial y} = 0$$

$$c' = \sqrt{\frac{k'}{m}\frac{M^2}{h_{co}^2} - \beta + 1}$$

where p^* is the pressure in the porous matrix, , h_{co} denotes the initial minimum film height, k' be the permeability of porous facing, m porosity and β being non dimensional minimum film thickness.

The relevant boundary condition for the velocity components are

$$u = 0, v = 0 \text{ at } y = 0 \tag{6}$$

$$u=0, v = \frac{\partial h_c}{\partial t} \quad \text{at } y = h \tag{7}$$

$$\frac{\partial^2 u}{\partial y^2} = 0 \text{ at } y = 0 \text{ \& } y = h \tag{8}$$

The conditions in Eqs (6) and (7) are the conventional non-slip conditions. The condition in Equ (7) comes from the vanishing of couple stresses at the solid boundary [11]. Applying the boundary conditions Eqs (6) and (8), the velocity component in the r-direction is obtained by integrating Eqn (2).

$$u = -\frac{h_{co}^2}{\left(E_1^2 - E_2^2\right)M^2\mu}\left(\frac{\partial p}{\partial r}\right)\left\{E_2^2\frac{\cosh\left(E_2\left(y-\frac{h}{2}\right)\right)}{\cosh\left(\frac{E_2 h}{2}\right)} - E_1^2\frac{\cosh\left(E_1\left(y-\frac{h}{2}\right)\right)}{\cosh\left(\frac{E_1 h}{2}\right)} + \left(E_1^2 - E_2^2\right)\right\} \quad (9)$$

where

$$M = B_o h_{co}\sqrt{\frac{\sigma}{\mu}} \quad (10)$$

$$l = \sqrt{\frac{\eta}{\mu}} \quad (11)$$

$$N = \frac{l}{h_{co}} \quad (12)$$

$$E_1 = \frac{\sqrt{1+\sqrt{1-4M^2N^2}}}{\sqrt{2}N} \quad (13)$$

$$E_2 = \frac{\sqrt{1-\sqrt{1-4M^2N^2}}}{\sqrt{2}N} \quad (14)$$

Also, h_{co} denotes the initial minimum film height and M describes the magnetization Hartmann number parameter measuring the strength of applied magnetic field. Since the dimension of *l* defined in Eq (11) is of length, it can be identified as the characteristics material length of the suspended particles. Therefore the non-Newtonian influences on the squeeze film are characterized by the non-Newtonian parameter of couple stress, N.

Integrating the continuity equation (4) across the film thickness gives

$$\frac{1}{r}\int_{y=0}^{h}\frac{\partial(ru)}{\partial r}dy = -\int_{y=0}^{h}\frac{\partial v}{\partial y}dy \quad (15)$$

Substituting the expression of the velocity component eqn (9) and applying the boundary condition (6) and (7), the MHNN Reynolds equation for the curved circular porous squeeze film plates can be derived.

$$\frac{1}{r}\frac{d}{dr}\left\{f(M,N,h)r\frac{dp}{dr}\right\} = 12\mu\frac{dh_c}{dt}$$

where

$$f(M,N,h) = \frac{12h}{M^2}\left\{1-2\left[\frac{E_1^3\tanh\left(\frac{E_2 h}{2}\right)+E_2^3\tanh\left(\frac{E_1 h}{2}\right)}{E_1E_2(E_1^2-E_2^2)h}\right]\right\} \quad (16)$$

To analyze the porous squeeze film characteristics, the MHNN Reynolds equation is expressed in a non-dimensional form.

$$\frac{1}{r^*}\frac{d}{dr^*}\left\{f^*(M,N,h^*)r^*\frac{dp^*}{dr^*}\right\} = -12 \quad (17)$$

$$f(M,N,h^*) = \frac{12h^*}{M^2}\left\{1-2\left[\frac{E_1^3\tanh\left(\frac{E_2 h^*}{2}\right)+E_2^3\tanh\left(\frac{E_1 h^*}{2}\right)}{E_1E_2(E_1^2-E_2^2)h^*}\right]\right\} \quad (18)$$

where

$$h^* = \frac{h}{h_{co}} = h_c^*\exp(-kr^{*^2})$$

$$r^* = \frac{r}{a}, h_c^* = \frac{h_c}{h_{co}}, p^* = \frac{ph_{co}^3}{\mu a^2\left(-\frac{dh_c}{dt}\right)}$$

The non-dimensional film pressure can be derived by solving the MHD non-Newtonian Reynolds equation (17) subject to the boundary conditions

$$\frac{dp^*}{dr} = 0 \quad \text{at } r=0 \text{ and } P^* = 0 \text{ at } r^* = 1$$

$$P^* = 6\int_{r^*=r^*}^{r^*=1}\frac{r^*}{f^*\left(M.N,h^*\right)}dr^* \quad (19)$$

Integrating the film pressure over the film region, the load carrying capacity is obtained

$$W = 2\pi \int_{r=0}^{a} prdr \tag{20}$$

Performing the integration, the non-dimensional load-carrying capacity is then expressed as the follows:

$$W^* = \frac{Wh_{co}^3}{\mu a^4\left(-\frac{dh_c}{dt}\right)} = 6\pi \int_{r^*=0}^{1} \frac{r^{*3}}{f^*\left(M,N,h^*\right)} dr^* \tag{21}$$

Introduce a non-dimensional approaching time for the porous curved circular squeeze film, $T^* = \frac{wh_{co}^2}{\mu a^4} T$. Then the differential equation governing the porous film thickness changing with the approaching time can be derived from equation (21).

$$\frac{dh_c^*}{dt} = -\left[6\pi \int_{r^*=0}^{1} \frac{r^{*3}}{f^*\left(M,N,h^*\right)} dr\right]^{-1} \tag{22}$$

Integrating the differential equation and applying the initial condition $h_c^*\left(T^*=0\right)=1$, the non-dimensional approaching time for the squeeze film is obtained.

$$T^* = \int_{h_c^*}^{h_c^*=1} \int_{r^*=0}^{1} \frac{r^{*3}}{f^*\left(M.N,h^*\right)} dr^* dh_c^* \tag{23}$$

The above integrations are solved by using Gaussian Quadrature Method.

3. RESULTS AND DISCUSSIONS

According to the present study, Figure-2 represents Newtonian case of parallel circular porous squeeze film when $M \to 0, N \to 0$. It shows that squeeze film shapes of exponential curved circular plates for different values of the shape parameter k. For k<0, convex films are obtained. For k>0, concave films are generated. For k=0, the geometry between parallel circular plates is recoverd as Hamrock [9]. The non-dimensional function derived in the Reynolds equation (17) reduces to the identical results by Hamrock [9].

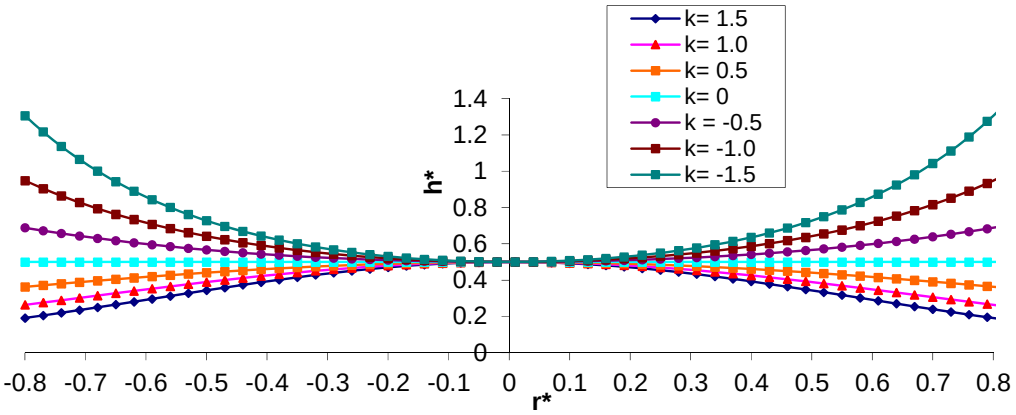

Figure-2. Newtonian (N) Squeeze film shapes of exponential curved plates for different values of the shape parameter *k* under $h_c^*=0.5$, $M=0$ and non-Newtonian parameter of couple stresses $N=0$.

Figure-3 shows non-dimensional pressure distribution p^* for the parameter $M \neq 0, N \to 0, k \neq 0$. It represents the MHD case of porous curved circular squeeze films. The reduced non-dimensional function f^* is the same as the one derived by Lin *et al* [3], in which the curved annular plates using Equation (1) are investigated.

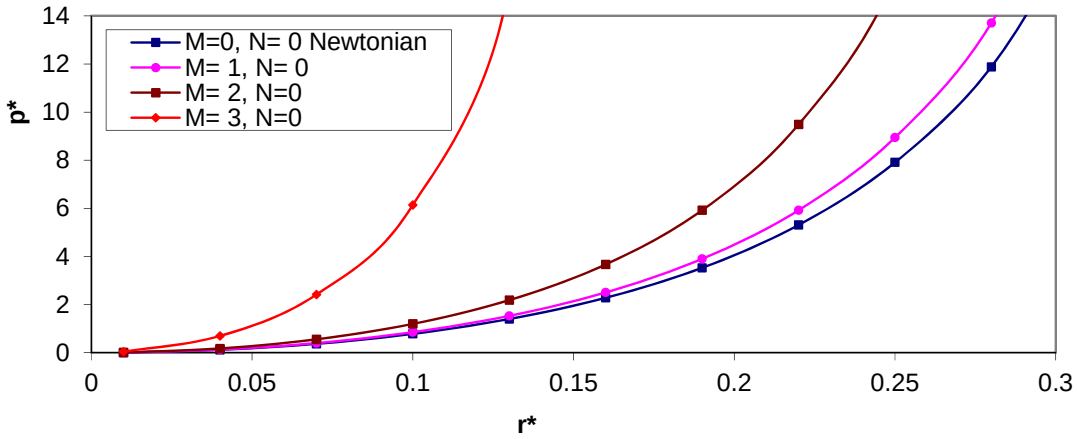

Figure-3. MHD Non-dimensional Pressure p^* as a function of r^* for different values of Hartmann Number M under $h_c^*=0.5$ and non-Newtonian parameter of couple stresses $N=0$.

Figure-4 shows non-dimensional pressure distribution p^* for the parameter $M \neq 0, N = 0.08, k \neq 0.$ It represents the MHNN case of porous curved circular squeeze films. Figure-5 shows MHNN non-dimensional pressure distribution p^* for the parameter $M \neq 0, N = 0.1, k \neq 0$.

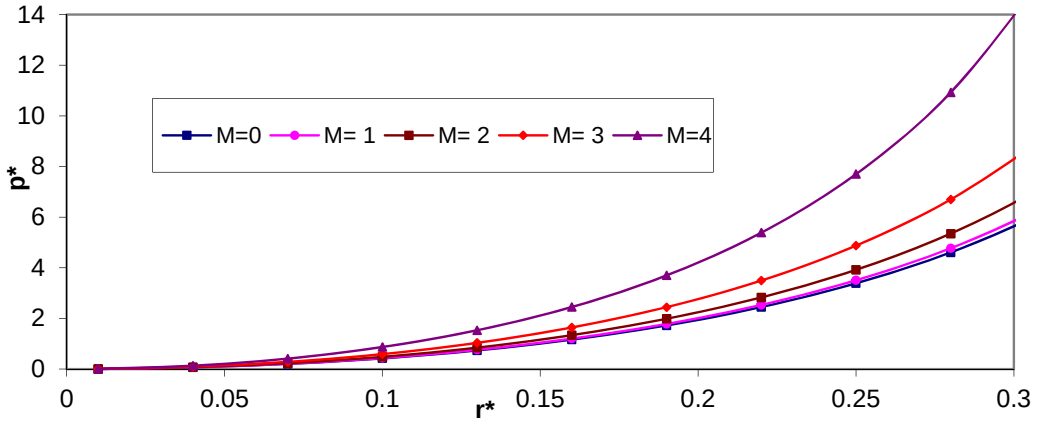

Figure-4. MHNN Non-dimensional Pressure p^* as a function of r^* for different values of Hartmann Number M under $h_c^*=0.5$ and non-Newtonian parameter of couple stresses $N=0.08$.

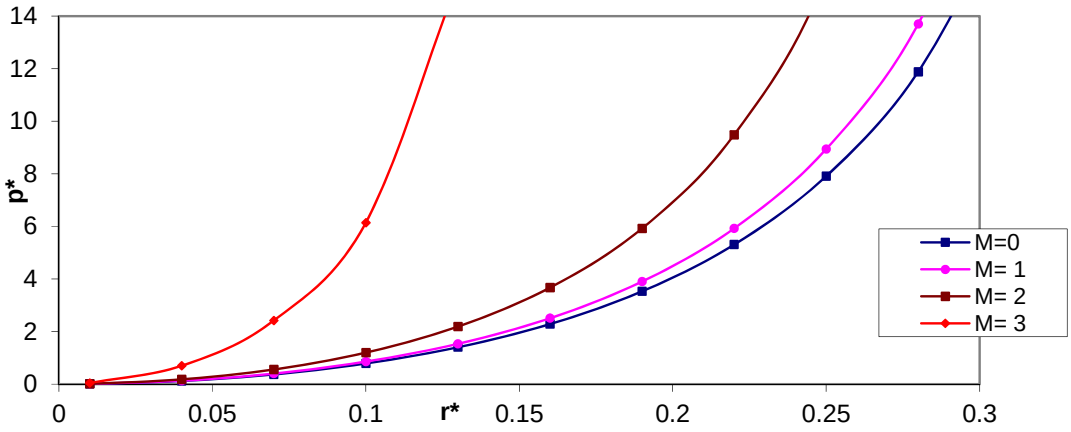

Figure-5. MHNN Non-dimensional Pressure p^* as a function of r^* for different values of Hartmann Number M under $h_c^*=0.5$ and non-Newtonian parameter of couple stresses $N=0.1$.

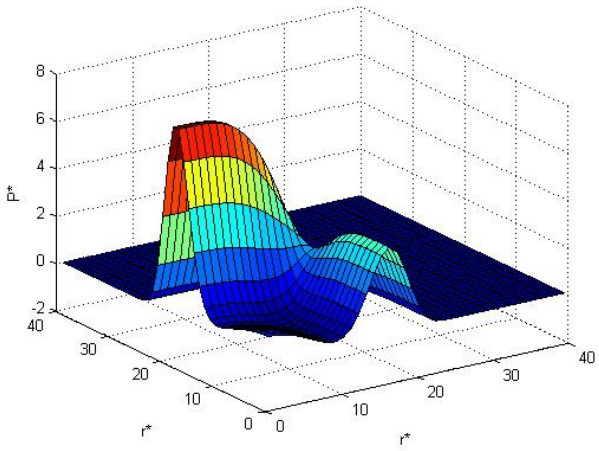

Figure-6(a). MHNN Non-dimensional Surface plot Pressure peaks p^* as a function of r^* for values of Hartmann Number M=1 under $h_c^*=0.5$, $k=1$ and non-Newtonian parameter of couple stresses $N=0.08$.

Figure-6(a) shows MHNN non-dimensional surface-plot pressure-peaks p^* for the Hartmann Number $M=1$ under non-Newtonian parameter of couple stresses, $N=0.08$ and $k=1$. Figure-6(b) shows MHNN non-dimensional surface-plot pressure-peaks p^* for the Hartmann Number $M=3$ under $N=0.08$ and $k=1$. Also, Figure-6(c) shows MHNN non-dimensional surface-plot pressure-peaks p^* for the Hartmann Number $M=5$ under $N=0.08$ and $k=1$.

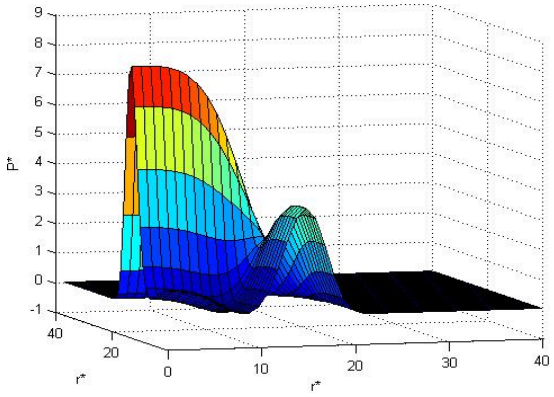

Figure-6(b). MHNN Non-dimensional Surface plot Pressure peaks p^* as a function of r^* for values of Hartmann Number M=3 under $h_c^*=0.5$, $k=1$ and non-Newtonian parameter of couple stresses $N=0.08$.

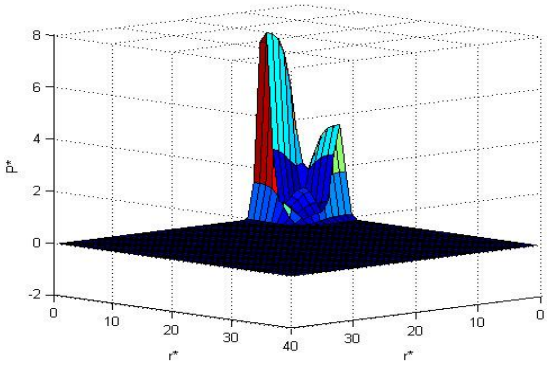

Figure-6(c). MHNN Non-dimensional Surface plot Pressure peaks p^* as a function of r^* for values of Hartmann Number M=5 under $h_c^*=0.5$, $k=1$ and non-Newtonian parameter of couple stresses $N=0.08$.

Figure-7(a) shows MHNN non-dimensional surface-plot pressure-peaks p^* for the Hartmann Number *M=1* under non-Newtonian parameter of couple stresses, *N=0.1* and *k=1.5*. Figure-7(b) shows MHNN non-dimensional surface-plot pressure-peaks p^* for the Hartmann Number *M=2* under *N=0.1* and *k=1.5*. Figure-7(c) shows MHNN non-dimensional surface-plot pressure-peaks p^* for the Hartmann Number *M=3* under *N=0.1* and *k=1.*5. At M=5 under *N=0.1* and *k=1.*5, Figure-7(d) shows maximum MHNN reaches solid and no pressure is involved.

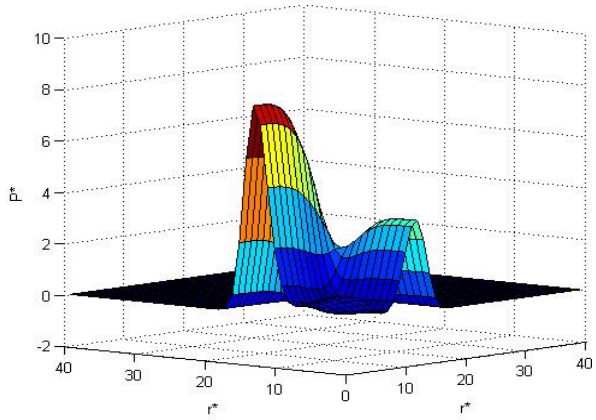

Figure-7(a). MHNN Non-dimensional Surface plot Pressure peaks *p** as a function of *r** for values of Hartmann Number M=1 under h_c^**=0.5, k=1.5* and non-Newtonian parameter of couple stresses *N=0.1*.

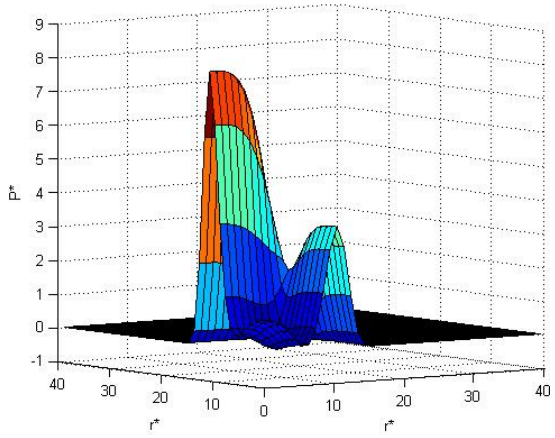

Figure-7(b). MHNN Non-dimensional Surface plot Pressure peaks *p** as a function of *r** for values of Hartmann Number M=2 under h_c^**=0.5, k=1.5* and non-Newtonian parameter of couple stresses *N=0.1*.

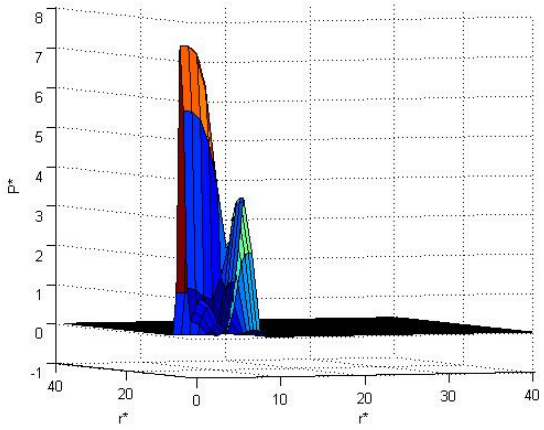

Figure-7(c). MHNN Non-dimensional Surface plot Pressure peaks *p** as a function of *r** for values of Hartmann Number M=3 under h_c^**=0.5, k=1.5* and non-Newtonian parameter of couple stresses *N=0.1*.

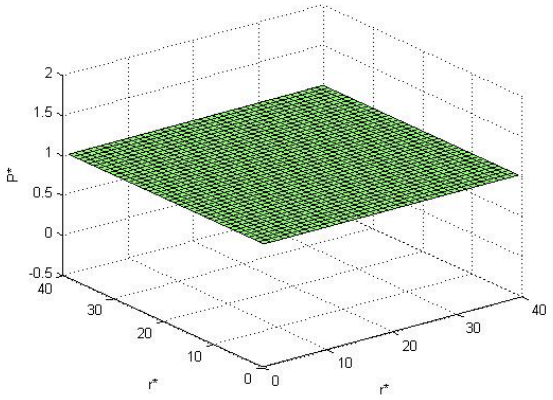

Figure-7 (d). Maximum MHNN Non-dimensional Surface plot Pressure peaks *p** as a function of *r** for values of Hartmann Number M=5 under h_c^**=0.5, k=1.5* and non-Newtonian parameter of couple stresses *N=0.1*.

Figure-8 shows the non-dimensional Load carrying capacity W^* as a function of r^* under h_c^**=0.5, k=1* and non-Newtonian parameter of couple stresses, *N=0* (Newtonian). The Newtonian case of N=0 and M=0 are plotted and compared with MHD case of $M \neq 0, N = 0$ and found that the values of the load-carrying capacity increases.

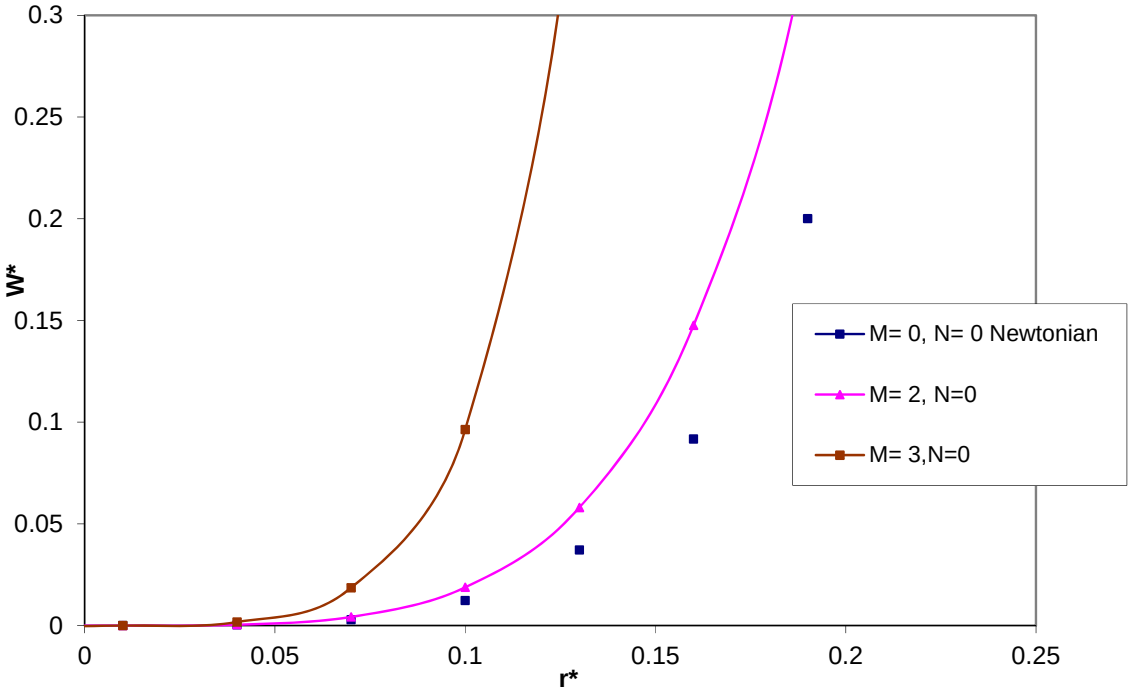

Figure-8. MHD Non-dimensional Load-carrying capacity W^* as a function of r^* for different values of Hartmann Number M under $h_c^*=0.5$ and non-Newtonian parameter of couple stresses $N=0$.

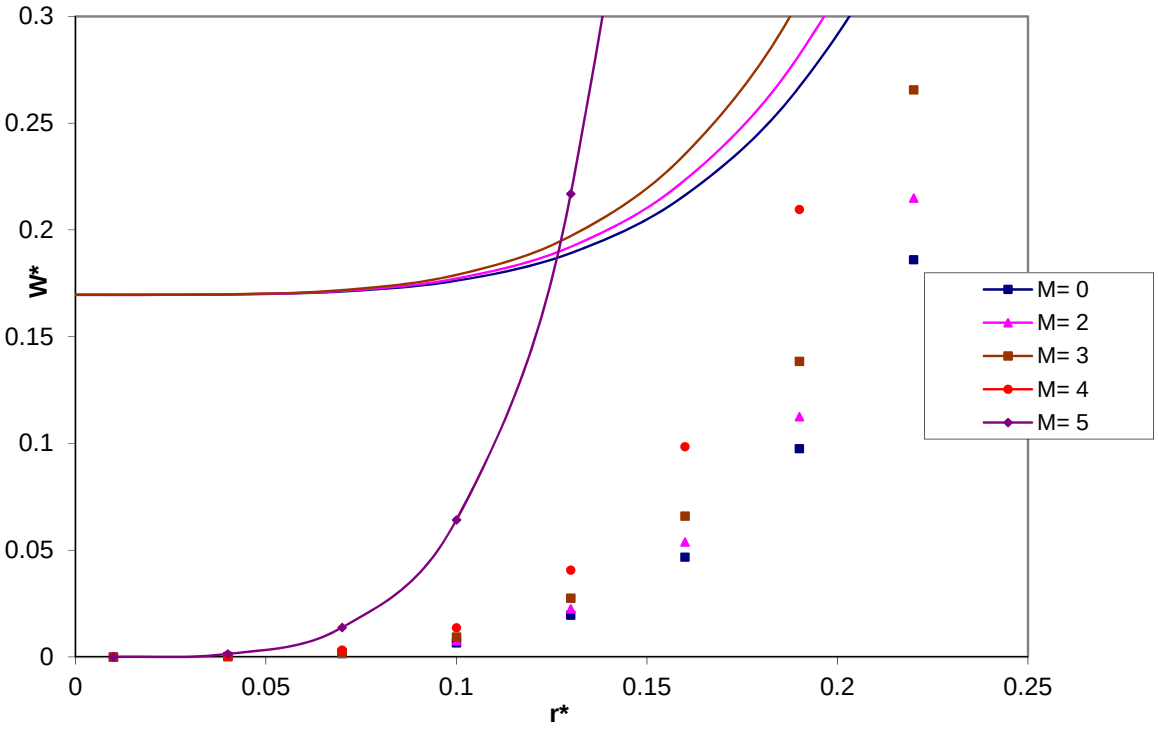

Figure-9. MHNN Non-dimensional Load-carrying capacity W^* as a function of r^* for different values of Hartmann Number M under $h_c^*=0.5$ and non-Newtonian parameter of couple stresses $N=0.08$.

Figure-9 shows the non-dimensional Load carrying capacity W^* as a function of r^* for different values of Hartmann Number, M under $h_c^*=0.5$, $k=1$ and non-Newtonian parameter of couple stresses, $N=0.08$. The non-Newtonian case of $N \neq 0$ and M=0 are plotted and compared with MHNN case of $M \neq 0, N = 0.08$ and found that the values of the load-carrying capacity increases.

Figure-10 shows the non-dimensional Load carrying capacity W^* as a function of r^* for different values of Hartmann Number, M under $h_c^*=0.5$, $k=1$ and non-Newtonian parameter of couple stresses, $N=0.1$. The non-Newtonian case of $N \neq 0$ and M=0 are plotted and compared with MHNN case of $M \neq 0, N = 0.1$ and found that the values of the load-carrying capacity increases. Increasing values of the couple-stress parameter (N=0.08, 0.1) increases the non-Newtonian effects on the load capacity. By the use of an electrically conducting non-Newtonian couple-stress fluid, the increments of the load capacity are enlarged. Totally, the MHNN effects on the porous squeeze film load are further emphasized for a larger value of the Hartmann parameter M, the non-Newtonian parameter N and the curved shape parameter k.

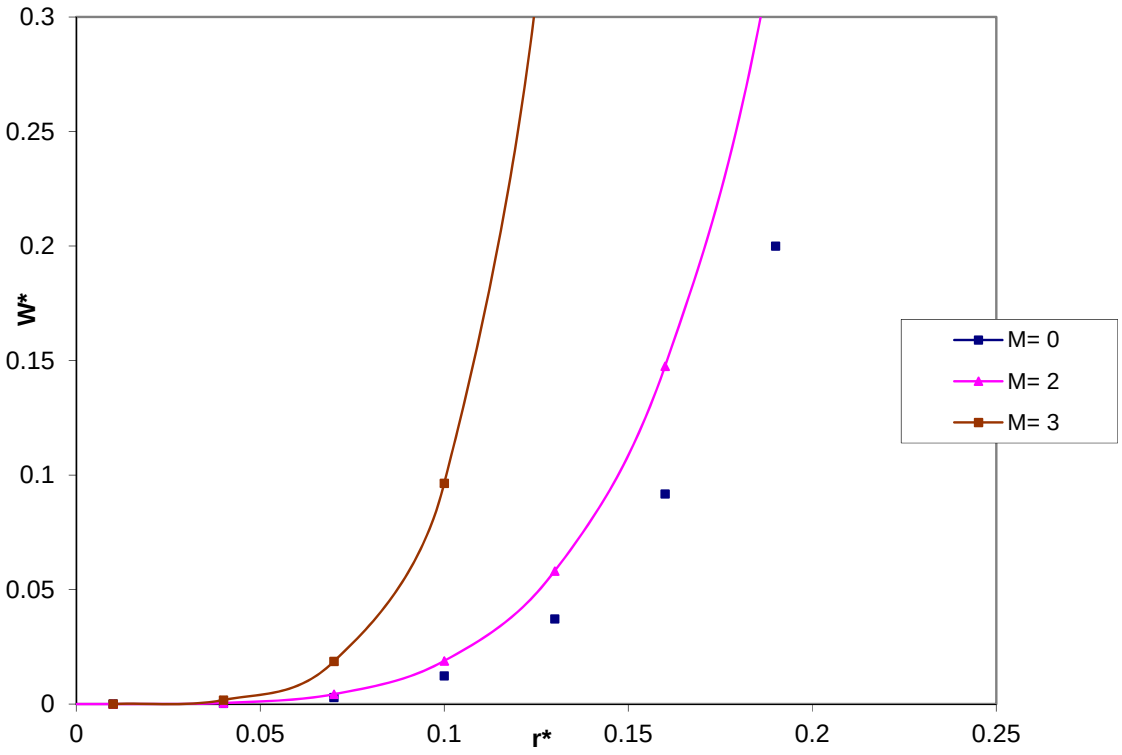

Figure-10. MHNN Non-dimensional Load-carrying capacity W^* as a function of r^* for different values of Hartmann Number M under $h_c^*=0.5$ and non-Newtonian parameter of couple stresses $N=0.1$.

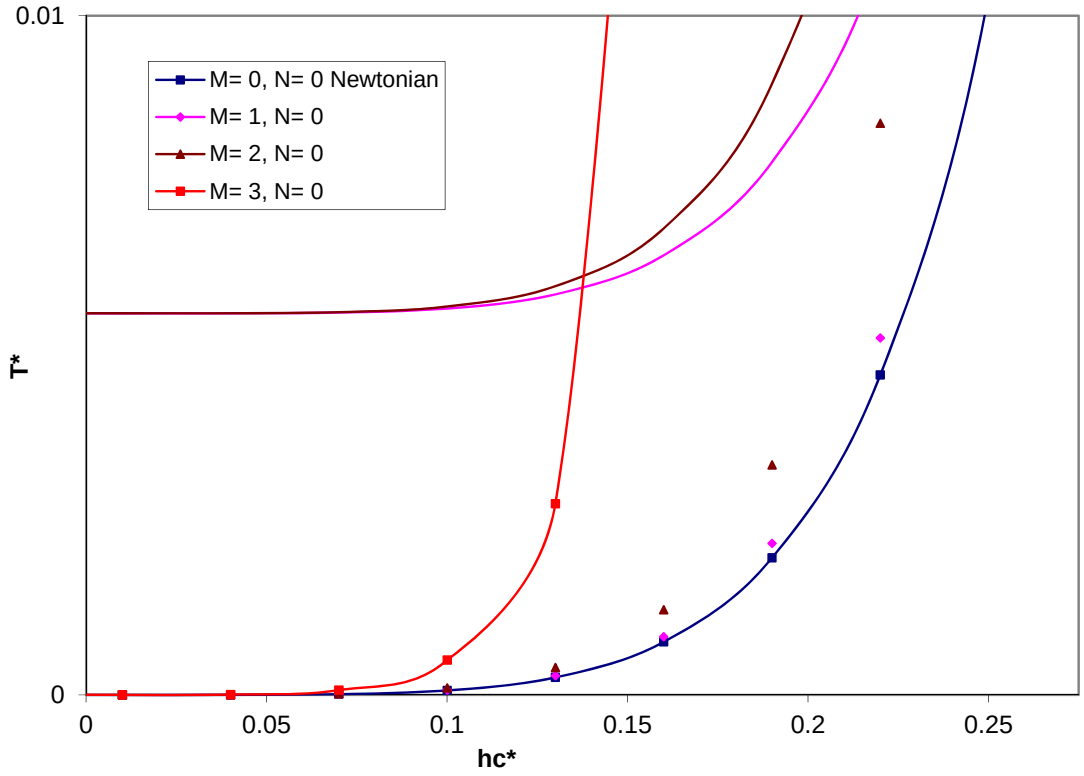

Figure-11. MHD Non-dimensional response time T^* as a function of h_c^* for different values of Hartmann Number M under non-Newtonian parameter of couple stresses $N=0$.

Figure-11 describes the MHD non-dimensional response time T^* as a function of h_c^*, $k=1$ and $N=0$ for different Hartmann Number M. The curved circular porous squeeze films lubricated with an electrically conducting non-Newtonian fluid effect are observed to provide an increase in the response time. Figure-12 describes MHNN the non-dimensional response time T^* as a function of h_c^*, $k=1$ and $N \neq 0$ $(N=0.08)$ for different Hartmann Number M. Figure-13 describes MHNN the non-dimensional response time T^* as a function of h_c^*, $k=1$ and $N \neq 0$ $(N=0.1)$ for different Hartmann Number M. Since MHNN effects result in a higher load-carrying capacity, a higher film thickness would be attained for the same time to be taken as compared to the Newtonian case. Therefore, a longer response time is predicted for the MHNN porous squeeze film. The response times of curved circular porous squeeze films are significantly lengthened by the use of an electrically conducting non-Newtonian fluid in the presence of external magnetic fields.

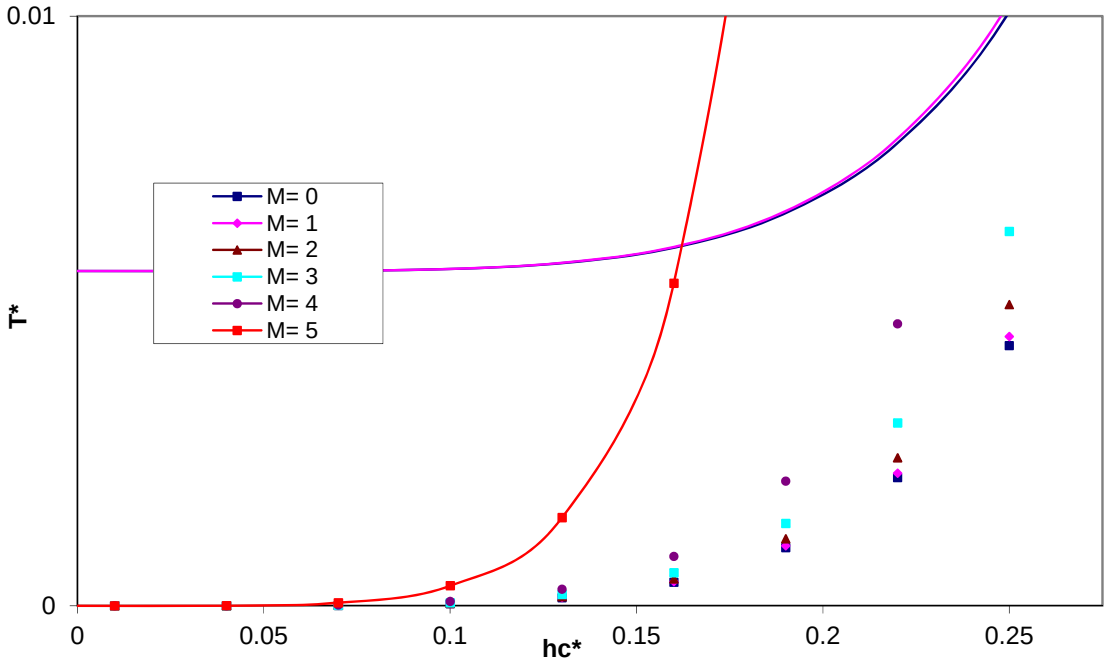

Figure-12. MHNN Non-dimensional response time T^* as a function of h_c^* for different values of Hartmann Number M under non-Newtonian parameter of couple stresses $N=0.08$.

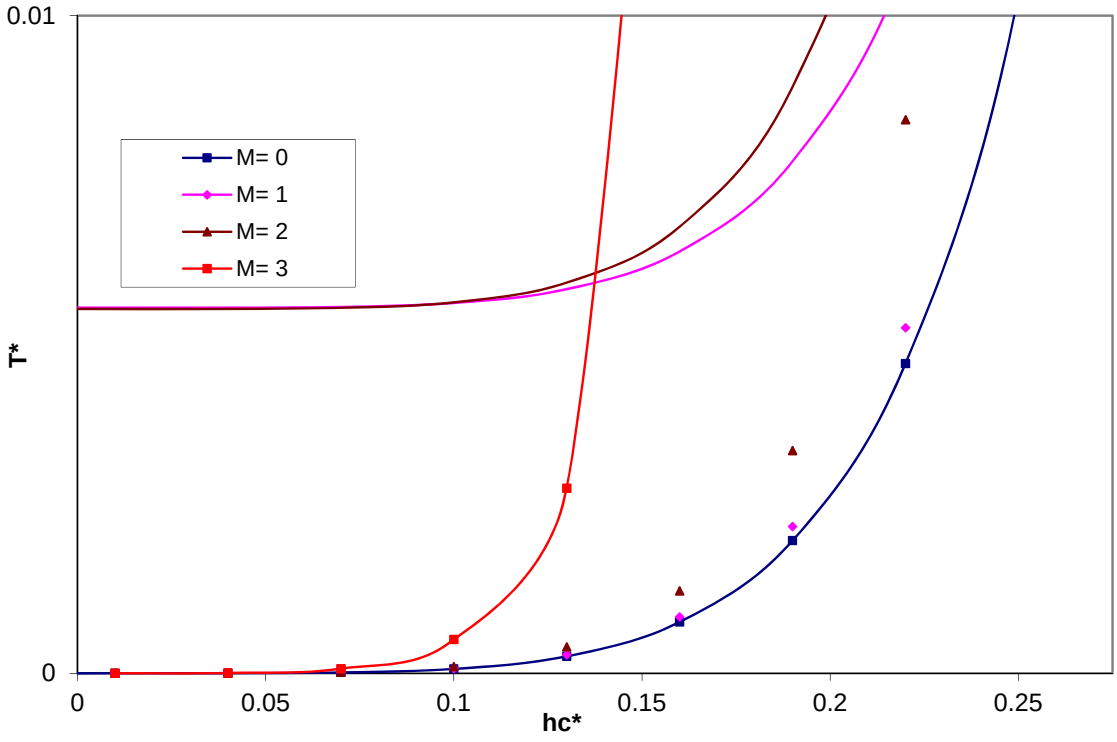

Figure-13. MHNN Non-dimensional response time T^* as a function of h_c^* for different values of Hartmann Number M under non-Newtonian parameter of couple stresses $N=0.1$.

Table-1. Comparison of the Porous MHD Load carrying capacity W^* and the Response time T^* with the Newtonian results under $h_c^*=0.5$, $k=1$ and $N = 0$.

r*	**Newtonian results Murti [8]**		**Porous squeeze film MHNN curved circular plates**					
			M = 0		***M = 1***		***M=2***	
	W^*	T^*	W^*	T^*	W^*	T^*	W^*	T^*
r=0.13*	0.039178	0.000257	0.039178	0.000257	0.040649	0.00028	0.058049	0.000401
r=0.16*	0.091736	0.000779	0.091736	0.000779	0.100764	0.000856	0.147541	0.001253
r=0.22*	0.403346	0.00471	0.403346	0.00471	0.449988	0.005255	0.720779	0.008417

Table-2. Comparison of the Porous MHNN Load carrying capacity W^* and the Response time T^* with the Newtonian results under $h_c^*=0.5$, $k=1$ and $N = 0.08$.

r*	**Newtonian results Murti** [8]		**Porous squeeze film MHNN curved circular plates**					
			M = 0		***M = 1***		***M = 2***	
	W^*	T^*	W^*	T^*	W^*	T^*	W^*	T^*
r=0.13*	0.19541	0.00135	0.19541	0.00135	0.20217	0.00140	0.22507	0.00155
r=0.16*	0.46690	0.00397	0.46690	0.00397	0.48301	0.00410	0.53814	0.00457
r=0.22*	1.86030	0.02172	1.86030	0.02172	1.90961	0.02249	2.14934	0.02510
			M = 3		*M = 4*		*M = 5*	
			W^*	T^*	W^*	T^*	W^*	T^*
			0.27526	0.00190	0.40662	0.00281	2.16883	0.01497
			0.65978	0.00560	0.98981	0.00836	6.44054	0.05470
			2.65587	0.03101	4.09357	0.04780	9.04793	1.05655

Table-3. Comparison of the Porous MHNN Load carrying capacity W^* and the Response time T^* with the Newtonian results under $h_c^*=0.5$, $k=1$ and $N = 0.1$.

r*	**Newtonian results Murti** [8]		**Porous squeeze film MHNN curved circular plates**					
			M = 0		***M = 1***		***M=2***	
	W^*	T^*	W^*	T^*	W^*	T^*	W^*	T^*
r=0.13*	0.37178	0.000257	0.37178	0.000257	4.06490	0.000280	5.801900	0.000401
r=0.16*	0.91736	0.000779	0.91736	0.000779	10.0764	0.000856	14.75410	0.001253
r=0.22*	4.03346	0.004710	4.03346	0.004710	44.9988	0.005255	72.07790	0.008417

The squeeze film characteristics for porous curved circular plates are improved by the use of an electrically conducting non-Newtonian fluid in the presence of external magnetic fields as compared to the case of Newtonian squeeze film results of Murti [8] are illustrated in the Tables 1, 2 and 3. Table values illustrate the MHNN load capacity and the MHNN approaching time of porous curved circular squeeze films are improved for higher values of magnetic Hartmann Number *M*.

CONCLUSIONS

Comparing with the conventional Newtonian case, the MHNN curved circular porous squeeze film characteristics are improved by the use of an electrically conducting non-Newtonian fluid in the presence of external magnetic fields.

Nomenclature	
a radius of curved circular plate	r,y radial and axial coordinates
B_o applied magnetic field	u,v Velocity components of the fluid in the film region
h_c central minimum film thickness at t=0	u^*,v^* Velocity components of the fluid in the porous region
h_{co} initial minimum film height	T Squeeze time
H_o porous bearing of wall thickness	T^* Non-dimensional squeeze time
k curved shape parameter	W Load-carrying capacity
k' permeability of the porous material	W^* Non-dimensional load-carrying capacity
m porosity	μ Lubricant viscosity
M Magnetic Hartmann number	σ Electrical conductivity
N Non-Newtonian parameter of couple-stress	η Material constant
p hydrodynamic film pressure	
p^* pressure in porous matrix	
P^* Non-dimensional film pressure	

REFERENCES

[1] Malik M. and Singh D.V. 1980. Analysis of finite MHD journal bearings, Wear. 64: 273-280.

[2] Lin J.R. 2010. MHD steady and dynamic characteristics for wide tapered-land slider beaings. Tribology International. 43: 2378-2383.

[3] Lin J.R., Lu, R.F. and Liao W.H. 2004. Analysis of MHD squeeze film characteristics between curved annular plates. Industrial Lubrication and Tribology. 56: 300-305.

[4] Oliver D.R. 1988. Load enhancement effects due to polymer thickening in a short model journal bearing. Journal of Non-Newtonian Fluid Mechanics. 30: 185-189.

[5] Ahmad N and Singh J.P. 2007. A model for couple-stress fluid film mechanism with reference to human joints. Proceedings of the Institution of Mechanical Engineers: Journal of Engineering Tribology. 221: 755-759.

[6] Elsharkawy A.A. and AL-Fadhalah K.I. 2008. Seperation of a sphere from a flat in the presence of couple stress fluids. Lubrication Science. 20: 61-74.

[7] Lin J.R., Chu L.M. and Lu R.F. 2014. MHNN curved circular squeeze films. Journal of Marine Science and Technology. 22(5): 566-571.

[8] Murti P.R.K. 1975. Squeeze films in curved circular plates. ASME Journal of Lubrication Technology. 97: 650-652.

[9] Hamrock B.J. 1994. Fundamentals of Fluid Film Lubrication. McGraw-Hill. pp. 286-287.

[10] Stokes V.K. 1966. Couple stresses in fluid. Physics of Fluids. 9: 1709-1715.

[11] Sundarammal K., Ali. J. Chamkha and Santhana Krishnan N. 2014. MHD squeezes film characteristics between finite porous parallel rectangular plates with surface roughness. International journal of Numerical methods for heat and fluid flow. 24(7): 1595-1609.